Mitigating cellular interference in uplink UAV communications

Tan, Ernest Zheng Hui; Madhukumar, A.S.; Sirigina, Rajendra Prasad; Krishna, Anoop Kumar

2021

Tan, E. Z. H., Madhukumar, A. S., Sirigina, R. P., & Krishna, A. K. (2021). Mitigating cellular interference in uplink UAV communications: Proceedings of 2020 IEEE 92nd Vehicular Technology Conference (VTC2020-Fall). doi:10.1109/VTC2020-Fall49728.2020.9348598

https://hdl.handle.net/10356/146720

https://doi.org/10.1109/VTC2020-Fall49728.2020.9348598

Mitigating Cellular Interference in Uplink UAV Communications

Tan Zheng Hui Ernest*, A S Madhukumar*, Rajendra Prasad Sirigina*, Anoop Kumar Krishna**
*School of Computer Science and Engineering
Nanyang Technological University, Singapore
Email: tanz0119@e.ntu.edu.sg, {raje0015, asmadhukumar}@ntu.edu.sg
**Airbus Singapore Pte Ltd, Singapore
Email: anoopkumar.krishna@airbus.com

***Abstract*—In this paper, we demonstrate the necessity of robust cellular interference cancellation when co-locating uplink (UL) unmanned aerial vehicle (UAV) communications with cellular networks. Through a stochastic geometry based evaluation framework, we show through bit error rate (BER) and ergodic capacity analysis that multi-user interference (MUI) is the main limiting factor in UL UAV communications after cellular interference cancellation. It is also observed that high altitudes and weak residual cellular interference corresponds to lower BER. In contrast, low altitudes and weak residual cellular interference results in higher ergodic capacity. Hence, advanced interference cancellation techniques should be considered to suppress the presence of strong MUI in the multi-UAV network.**

***Index Terms*—Unmanned Aerial Vehicle, Bit Error Rate, Ergodic Capacity, Rician Fading, Stochastic Geometry.**

I. Introduction

In recent years, the deployment of unmanned aerial vehicles (UAVs) for service delivery in future wireless networks, e.g., fifth generation (5G) networks, has garnered much interest in both industry and academia. While a wide variety of UAV applications are being considered, e.g., UAV-assisted relays [1], spectrum scarcity remains a major challenge towards supporting reliable and effective UAV communications [1].

In this context, capitalizing on existing cellular infrastructure to support multi-UAV networks is a subject of ongoing research. Although both cellular and multi-UAV networks are able to share the same time-frequency resource block, strong interference can be experienced in both multi-UAV and cellular networks. In the literature, power control [2] and cooperative interference cancellation [3] have been proposed to mitigate mutual interference between multi-UAV and cellular networks. However, the impact of cellular interference on UAV communications has not been extensively studied. Furthermore, related studies that have analyzed the effects of interference in cellular networks are not entirely applicable for UAV communications. For example, commonly assumed Rayleigh fading channels in cellular communications may not be appropriate for UAV communications where Rician fading channels are more likely to occur [1], [4]–[6]. Also, stochastic geometry tools used in cellular and multi-UAV networks are also different. For instance, Poisson point processes (PPPs) are used to model the spatial location of cellular BSs. Yet, PPPs are not suitable for multi-UAV networks, which uses binomial point processes (BPPs) to model the spatial locations of UAVs [6], [7]. [1]

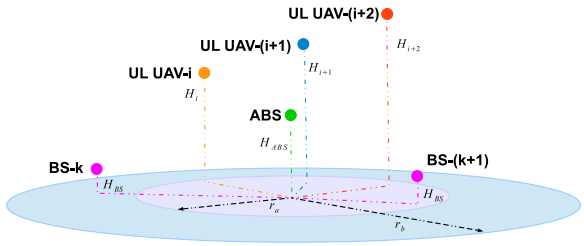

Fig. 1. An illustration of uplink UAV communications between the UL UAVs and the ABS is shown here. The ABS first cancels interference from nearby cellular BSs before detecting each of the UL UAV that are operating at different altitudes.

To this end, we investigate the effectiveness of canceling cellular interference in multi-UAV networks. The contributions of this paper are thus summarized as follows:

- A stochastic geometry based analytical method is proposed to characterized the impact of cellular interference mitigation on multi-UAV networks in terms of bit error rate (BER) and ergodic capacity at low-to-high transmit power regimes.
- Asymptotic BER, i.e., BER floor, and ergodic capacity expressions are also derived to capture the impact of residual cellular interference at asymptotic transmit power regimes.

The remainder of this paper is organized as follows. A detailed discussion on the the system model is provided in Section II, with BER and ergodic capacity derivations presented in Section III. Numerical results are then discussed in Section IV, before the paper concludes in Section V.

II. System Model

We consider a multi-UAV network with N_U UL UAVs and an aerial BS (ABS) operating in a suburban environment in the presence of interference from N_B cellular BSs (Fig. 1). For the N_U UAVs, N_B cellular BSs, and the ABS, single antenna transceivers are assumed. Furthermore, we assume

[1] In cellular networks, an infinite region is assumed when employing a PPP. However, such an assumption may not be practical for multi-UAV networks, which typically operate over a finite region [7].

transmissions from the UL UAVs and cellular BSs to occur over Rician fading channels due to the suburban environment [5], with Doppler shift compensated at the ABS.

A. Relevant Distance Distributions

To model the spatial location of the UL UAVs and interfering cellular BSs, the BPP-based model in [6], [7] is employed. [2] In particular, the spatial location of UL UAV-i is assumed to be uniformly distributed around a disc centered above the origin O with radius r_a, angle $[0, 2\pi)$, and altitude H_i [6], [7]. Likewise, the spatial locations of the cellular BSs are assumed to be uniformly distributed around a disc centered at the origin O with radius r_b, angle $[0, 2\pi)$, and height H_{BS}. Finally, we assume that the ABS is located at the center of the disc, i.e., origin O, at an altitude of H_{ABS}.

From the spatial locations of the UL UAVs, the Euclidean distance (km) between UL UAV-i and the ABS is $d_i = \sqrt{D_i^2 + \left(H_i - H_{ABS}\right)^2}$, where D_i denotes the Euclidean distance between the projection of UL UAV-i onto the ground plane and the ABS, $H_i = 2H_{ABS} - H_{BS} + \frac{i}{N_U}$, and $H_{BS} > 2H_{ABS} - H_i$. The altitude H_i is chosen such that UL UAV-i is located further away from the ABS than the cellular BSs. From [6], [7], the probability density function (PDF) of d_i is:

$$f_{d_i}(w_i) = \frac{2w_i}{r_a^2}, \quad (1)$$

where $L_{m,i} \leq w_i \leq L_{p,i}$, $L_{m,i} = \sqrt{\left(H_i - H_{ABS}\right)^2}$ and $L_{p,i} = \sqrt{\left(H_i - H_{ABS}\right)^2 + r_a^2}$.

For the interfering cellular BSs, the Euclidean distance (km) between BS-k and the ABS is $d_k = \sqrt{D_k^2 + \left(H_{ABS} - H_{BS}\right)^2}$, where D_k is defined in the same manner as D_i. Similar to $f_{d_i}(w_i)$, the PDF of d_k is [6], [7]:

$$f_{d_k}(w_k) = \frac{2w_k}{r_b^2}, \quad (2)$$

where $T_{m,k} \leq w_k \leq T_{p,k}$, $T_{m,k} = \sqrt{\left(H_{ABS} - H_{BS}\right)^2}$ and $T_{p,k} = \sqrt{\left(H_{ABS} - H_{BS}\right)^2 + r_b^2}$.

As the interfering cellular BSs are located at the same height (H_{BS}), the ordered set of interfering cellular BS distances is denoted as $\left\{d_{(k)}\right\}_{k=1:N_B}$, where $d_{(k)}$ is the kth closest interfering cellular BS to the ABS. Let $U_k = d_{(k)}$, then the resulting PDF is presented in the following theorem:

Theorem 1: The PDF of U_k for the ordered set $\left\{d_{(k)}\right\}_{k=1:N_B}$ is:

$$f_{U_k}(u_k) = \frac{N_B!\left[F_{d_k}(u_k)\right]^{k-1}\left[1 - F_{d_k}(u_k)\right]^{N_B-k}}{(k-1)!(N_B-k)!} f_{d_k}(u_k), \quad (3)$$

where $F_{d_k}(x) = \frac{x^2 - T_{m,k}^2}{r_b^2}$ is the cumulative distribution function (CDF) of d_k and $T_{m,k} \leq u_k \leq T_{p,k}$.

Proof: The PDF $f_{U_k}(u_k)$ is obtained by applying [9, eq. (8-14)]. ■

[2] It is useful to note that the work in [8] applied BPPs to model the spatial location of nodes in cellular networks.

B. SIC Detection Process at the ABS

For signal detection at the ABS, we assume that the UL UAVs and interfering cellular BSs transmit binary phase shift keying (BPSK) symbols belonging to the set $\{+1, -1\}$. To recover the signal-of-interest (SOI), the ABS starts the detection process with UL UAV-i. In particular, the ABS first employs successive interference cancellation (SIC) to remove interference from the interfering BSs. Thereafter, the SOI of UL UAV-i is detected in the presence of residual cellular interference and multi-user interference (MUI) from the remaining $N_U - i$ UL UAVs. After detecting UL UAV-i, SIC is invoked again to remove the message of UL UAV-i from the received composite signal. The ABS repeats the SIC detection process until the desired messages from all UL UAVs are recovered.

At each iteration of the SIC detection process, the received instantaneous signal-to-interference-plus-noise ratio (SINR) of UL UAV-i at the ABS is:

$$SINR_i = \frac{X_i d_i^{-n}}{1 + \sum_{j=i+1}^{N_U} X_j d_j^{-n} + \sum_{k=1}^{N_B} Y_k U_k^{-n}}, \quad (4)$$

where n is the pathloss exponent, $X_i = P_t|h_i|^2$, $X_j = P_t|h_j|^2$, $Y_k = P_t\beta_k|h_k|^2$, P_t is the normalized transmit power, $h_x, x \in \{i, j\}$ is the channel between UL UAV-x and the ABS, h_k is the channel between BS-k and the ABS, and $0 \leq \beta_k \leq 1$ is the strength of the residual cellular interference after SIC [6]. The variables X_i, X_j, and Y_k are non-centered Chi-squared distributed random variables (RVs) with Rician K factor $K_x, x \in \{i, j, k\}$.

At high P_t regimes, $SINR_i$ reduces into the following instantaneous signal-to-interference ratio (SIR):

$$SIR_i = \frac{\overline{X}_i d_i^{-n}}{\sum_{j=i+1}^{N_U} \overline{X}_j d_j^{-n} + \sum_{k=1}^{N_B} \overline{Y}_k U_k^{-n}}, \quad (5)$$

where $\overline{X}_q = |h_q|^2$ for $q \in \{i, j\}$, and $\overline{Y}_k = \beta_k|h_k|^2$. The RVs, $\overline{X}_q, q \in \{i, j\}$ and $\overline{Y}_k$ are similarly defined as non-centered Chi-squared distributed RVs with respective Rician K factors $\overline{K}_x, x \in \{i, j, k\}$.

From the above framework, the BPSK BER and ergodic capacity of the considered multi-UAV network can be analyzed to determine the effectiveness of cellular interference mitigation.

III. Derivation of Bit Error Rate and Ergodic Capacity Expressions

In this section, BER and ergodic capacity expressions are presented for UL UAV-i. In particular, both the BER and ergodic capacity of UL UAV-i are analyzed under finite and asymptotic P_t regimes.

A. Bit Error Rate of Uplink UAV-i

The BPSK BER of UL UAV-i ($P_{b,i}$) is defined as $P_{b,i} = \frac{1}{2}E\left\{\text{erfc}\left(\sqrt{SINR_i}\right)\right\}$, where $E\{\bullet\}$ is the statistical expectation operator and $\text{erfc}(x)$ is the complimentary error function. As it stands, a direct evaluation of $E\left\{\text{erfc}\left(\sqrt{SINR_i}\right)\right\}$ in $P_{b,i}$

requires $(N_B + N_U - i + 1)$-fold numerical integrations [10], [11]. To avoid such a pitfall, a simple technique that averages $E\left\{\text{erfc}\left(\sqrt{SINR_i}\right)\right\}$ with a single integral was proposed in [10].

In what follows, the technique in [10] is employed to derive a semi-analytical expression for $P_{b,i}$ in the next theorem.

Theorem 2: The BPSK BER of UL UAV-i is:

$$P_{b,i} \approx \frac{1}{2} + \frac{1}{2}\int_{L_{m,i}}^{L_{p,i}} \int_0^{\infty} \sum_{q=0}^{K_{tr}} \frac{(K_i)^q \exp(-K_i)}{\Gamma(q+1)^2} g_{q+1}(z) \times \exp(-m_i z)\left(\prod_{j=i+1}^{N_U} \tau_j(m_i z)\right)\left(\prod_{k=1}^{N_B} \mu_k(m_i z)\right) f_{d_i}(w_i) dz dw_i, \quad (6)$$

where K_{tr} is the truncation order, $m_i = \frac{K_i+1}{P_t d_i^{-n}}$, and $\Gamma(\bullet)$ is the Gamma function. Also, let $M_Z(z) = \frac{1+K_z}{1+K_z+P_z z} \exp\left(\frac{-K_z P_z z}{1+K_z+P_z z}\right)$ be the moment generation function (MGF) of the RV Z with variance P_z and Rician K factor K_z [12, Table. I]. Then, the functions, $g_{q+1}(z)$, $\tau_j(z)$, and $\mu_k(z)$, are respectively defined as:

$$\begin{aligned} g_{q+1}(z) &= \frac{2\Gamma\left(q+\frac{3}{2}\right)}{\sqrt{\pi z}\Gamma\left(\frac{1}{2}\right)} {}_1F_1\left(q+\frac{3}{2}, \frac{3}{2}; -z\right), \\ \tau_j(z) &= \int_{L_{m,j}}^{L_{p,j}} M_{X_j}(z) f_{d_j}(w_j) dw_j, \\ \mu_k(z) &= \int_{T_{m,k}}^{T_{p,k}} M_{Y_k}(z) f_{U_k}(u_k) du_k, \end{aligned}$$

where ${}_1F_1(\bullet)$ representing the confluent Hypergeometric function [6].

Proof: The proof is provided in Appendix A. ∎

From Theorem 2, one can obtain the BPSK BER error floor of UL UAV-i. Specifically, at high P_t regimes, the asymptotic BPSK BER of UL UAV-i ($\overline{P}_{b,i}$) is defined as $\overline{P}_{b,i} = \frac{1}{2}E\left\{\text{erfc}\left(\sqrt{SIR_i}\right)\right\}$. In the following theorem, a semi-analytical expression for $\overline{P}_{b,i}$ is presented.

Theorem 3: The asymptotic BPSK BER of UL UAV-i is:

$$\overline{P}_{b,i} \approx \frac{1}{2} + \frac{1}{2}\int_{L_{m,i}}^{L_{p,i}} \int_0^{\infty} \sum_{q=0}^{K_{tr}} \frac{(K_i)^q \exp(-K_i)}{\Gamma(q+1)^2} g_{q+1}(z) \times \left(\prod_{j=i+1}^{N_U} \overline{\tau}_j(\overline{m}_i z)\right)\left(\prod_{k=1}^{N_B} \overline{\mu}_k(\overline{m}_i z)\right) f_{d_i}(w_i) dz dw_i, \quad (7)$$

where $\overline{m}_i = \frac{K_i+1}{d_i^{-n}}$ and the functions, $\overline{\tau}_j(z)$, and $\overline{\mu}_k(z)$, are respectively defined as:

$$\begin{aligned} \overline{\tau}_j(z) &= \int_{L_{m,j}}^{L_{p,j}} M_{\overline{X}_j}(z) f_{d_j}(w_j) dw_j, \\ \overline{\mu}_k(z) &= \int_{T_{m,k}}^{T_{p,k}} M_{\overline{Y}_k}(z) f_{U_k}(u_k) du_k. \end{aligned}$$

Proof: Applying the same technique in Appendix A yields (7). ∎

Using (6) and (7), one can characterize the BPSK BER of UL UAV-i within a stochastic geometry framework to reveal the effectiveness of cellular interference mitigation.

TABLE I
SIMULATION PARAMETERS

Parameter	Value
Number of UAVs and BSs	$N_U = 3$, $N_B = 2$
Rician K Factors	10 dB [5, Table V]
Normalized Transmit Power	0 dB $\leq P_t \leq$ 30 dB
Residual Cellular Interference	$\beta_k \in \{0.05^2, 0.09^2\}$
Radius	$r_a = 4$ km, $r_b = 8$ km
ABS Altitude	$H_{ABS} \in \{0.7 \text{ km}, 4.7 \text{ km}\}$
BS Altitude	$H_{BS} = 0.01$ km
Pathloss Exponent	$n = 2$ [5, Table III]

B. Ergodic Capacity of Uplink UAV-i

The ergodic capacity of UL UAV-i (C_i) is defined as $C_i = E\left\{\ln\left(1+SINR_i\right)\right\}$. As a direct evaluation of the ergodic capacity in the presence of cellular interference also requires $(N_B + N_U - i + 1)$-fold numerical integrations [10], [11], we present a semi-analytical expression for C_i using the method proposed in [10] in the following theorem.

Theorem 4: The ergodic capacity of UL UAV-i is:

$$C_i \approx \int_{L_{m,i}}^{L_{p,i}} \int_0^{\infty} \frac{\exp(-z)}{z}\left[1 - M_{X_i}(z)\right] \times \left(\prod_{j=i+1}^{N_U} \tau_j(z)\right)\left(\prod_{k=1}^{N_B} \mu_k(z)\right) f_{d_i}(w_i) dz dw_i, \quad (8)$$

Proof: The proof is provided in Appendix B. ∎

Similar to Theorem 2, one can also obtain the asymptotic ergodic capacity of UL UAV-i. In particular, the asymptotic ergodic capacity ($\overline{C}_i$) is defined as $\overline{C}_i = E\left\{\ln\left(1+SIR_i\right)\right\}$. In the following theorem, a semi-analytical expression for $\overline{C}_i$ is presented.

Theorem 5: The asymptotic ergodic capacity of UL UAV-i is:

$$\overline{C}_i \approx \int_{L_{m,i}}^{L_{p,i}} \int_0^{\infty} \frac{1}{z}\left[1 - M_{\overline{X}_i}(z)\right] \times \left(\prod_{j=i+1}^{N_U} \overline{\tau}_j(z)\right)\left(\prod_{k=1}^{N_B} \overline{\mu}_k(z)\right) f_{d_i}(w_i) dz dw_i, \quad (9)$$

Proof: Employing the same technique in Appendix B yields (9). ∎

Using (4) and (5), the impact of cellular interference mitigation can be analzyed for the multi-UAV network.

IV. NUMERICAL RESULTS

In this section, we present numerical and simulation results for the BPSK BER and ergodic capacity in the multi-UAV network. The parameters are provided in Table I, with Monte Carlo simulations conducted using 10^7 samples.

In Fig. 2, the BPSK BER and asymptotic BPSK BER of UL UAV-i, i.e., $P_{b,i}$ and $\overline{P}_{b,i}$, are plotted. For UL UAV-$i, i \in \{1,2\}$, $P_{b,1}$ and $P_{b,2}$ are similar when the ABS altitude (H_{ABS}) is changed. In particular, the BPSK BER trend is due to the ABS SIC detection process being limited by MUI from the remaining UL UAVs. Thus, varying H_{ABS} does not

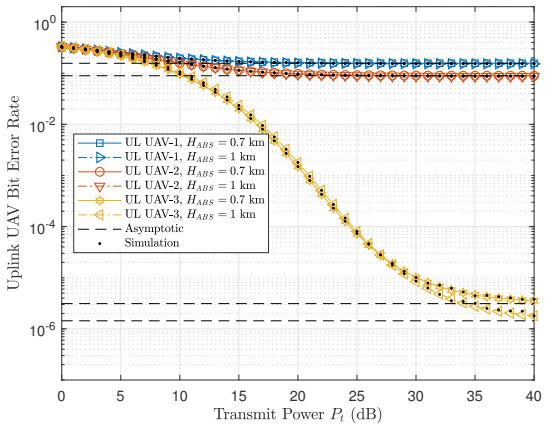

Fig. 2. Impact of H_{ABS} on BPSK BER in the multi-UAV network for $\beta_k = 0.05^2$.

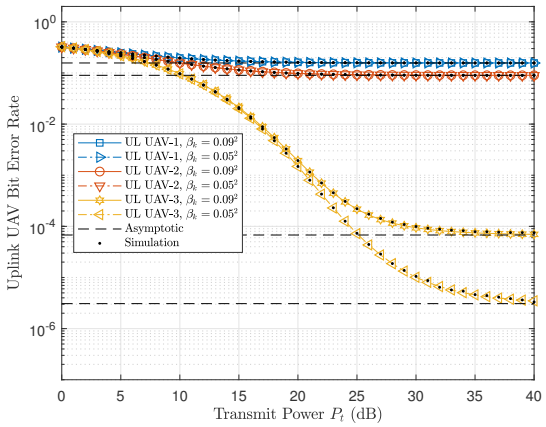

Fig. 3. Impact of β_k on BPSK BER in the multi-UAV network for $H_{ABS} = 0.7$ km.

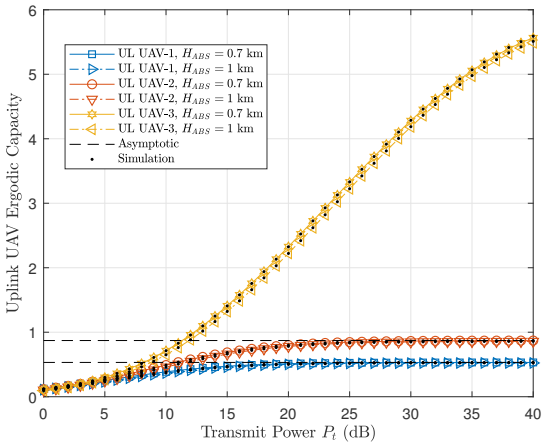

Fig. 4. Impact of H_{ABS} on BPSK BER in the multi-UAV network for $\beta_k = 0.05^2$.

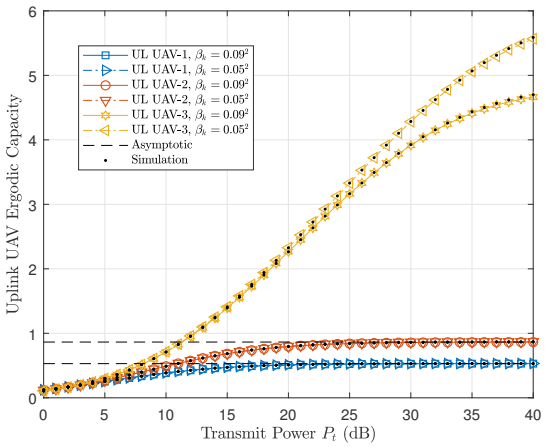

Fig. 5. Impact of β_k on BPSK BER in the multi-UAV network for $H_{ABS} = 0.7$ km.

effect any significant change in $P_{b,i}, i \in \{1,2\}$. For the case of UL UAV-3, increasing H_{ABS} also leads to an increase in the altitude of UL UAV-3 (H_3). Thus, increasing H_{ABS} also leads to higher $P_{b,3}$ when $P_t \leq 25$ dB. At high P_t regimes, i.e., $P_t > 25$ dB, the ABS SIC detection process for UL UAV-3 becomes limited by residual cellular interference. Hence, increasing H_{ABS} results in lower $P_{b,3}$ at high P_t regimes.

Similar results are also observed in Fig. 3 for UL UAV-$i, i \in \{1,2\}$. In particular, since the ABS SIC detection process is limited by MUI for UL UAV-$i, i \in \{1,2\}$, varying the strength of residual cellular interference (β_k) does not affect $P_{b,1}$ and $P_{b,2}$. In contrast, increasing β_k leads to higher $P_{b,3}$ at moderate-to-high P_t regimes, i.e., $P_t > 15$ dB. Specifically, it is observed that setting $\beta_k = 0.09^2$ leads to $P_{b,3}$ approaching the asymptotic BPSK BER ($\overline{P}_{b,3}$) at $P_t > 25$ dB.

In terms of ergodic capacity (C_i), it is seen in Fig. 4 that $C_i, i \in \{1,2\}$ approaches the asymptotic ergodic capacity $\overline{C}_i$ at high P_t regimes as the SIC detection process at the ABS is limited by MUI. In contrast, C_3 is only affected by residual cellular interference and not MUI-limited for 0 dB $\leq P_t \leq$ 30 dB. It is also observed that increasing H_{ABS} decreases C_i for the UL UAVs. Since increasing H_{ABS} leads to higher H_i, operating at higher H_{ABS} causes the UL UAVs to be further from the ABS. In turn, the strength of the SOI becomes weaker, resulting in lower C_i.

The impact of residual cellular interference on C_i is seen in Fig. 5. For UL UAV-$i, i \in \{1,2\}$, β_k does not affect C_i. However, it is observed that C_3 begins to plateau at high P_t regimes, i.e., $P_t > 25$ dB, when $\beta_k = 0.09^2$ as the SIC detection process at the ABS is limited by residual cellular interference.

Through the above BER and ergodic capacity analysis, operating multi-UAV networks in the presence of cellular interference requires effective and robust interference cancellation techniques. Furthermore, the strength of residual cellular interference can adversely affect reliability and throughput at high P_t regimes. To this end, other advanced interference cancellation techniques, e.g., interference forwarding, may have to be considered to suppress strong MUI and cellular interference in the multi-UAV network.

V. Conclusion

The effectiveness of employing SIC for cellular interference mitigation in a multi-UAV network with N_U UAVs is investigated in this work. Through an extensive analysis of the BER and ergodic capacity, we show that the SIC detection process for UL UAV-$i, i < N_U$ is limited by MUI across low-to-high transmit power regimes. In contrast, the SIC detection process for UL UAV-$i, i = N_U$ is limited by residual cellular interference and the ABS altitude. Specifically, it is observed that high ABS altitude and weak residual cellular interference leads to lower BER. For ergodic capacity, better performance is noted for low ABS altitude and weak residual cellular interference. Thus, we demonstrate the necessity of effective cellular interference cancellation for multi-UAV networks that are supported through cellular infrastructure.

Acknowledgment

This research is jointly funded by Airbus Singapore Pte Ltd and the Singapore Economic Development Board (EDB).

Appendix A
Proof of Theorem 2

We start by first letting $\mathcal{I} = \sum_{j=i+1}^{N_U} X_j d_j^{-n} + \sum_{k=1}^{N_B} Y_k U_k^{-n}$ and $z = \frac{X_i d_i^{-n}}{1+\mathcal{I}}$. Next, from [13, Table I] and [14, eq. (9.6.10)], we note that the PDF of X_i can be expressed as:

$$f_{X_i}(x_i) = \sum_{q=0}^{K_{tr}} \frac{(K_i)^q \exp(-K_i)}{\Gamma(q+1)^2} m_i^{q+1} x_i^q \exp(-m_i x_i), \quad (10)$$

where $I_0(\cdot)$ is the modified Bessel function of the first kind with zero order [14, eq. (9.6.10)].

For $g(z) = \operatorname{erfc}(\sqrt{z})$ and $g_k(z) = \frac{d^k}{dz^k} g(z) z^q$, it is straightforward to see that:

$$g_k(0) = \begin{cases} 0, & \text{for } k < q \\ g(0), & \text{for } k = q. \end{cases} \quad (11)$$

Also, from [10, eq. (9)], $\operatorname{erfc}(z) = 1 - \frac{2z}{\sqrt{z}} {}_1F_1\left(\frac{1}{2}, \frac{3}{2}; -z^2\right)$. Therefore, evaluating $g_{q+1}(z)$ yields:

$$\begin{aligned} g_{q+1}(z) &= \frac{-2}{\sqrt{\pi}} \frac{d^{q+1}}{dz^{q+1}} z^{q+\frac{1}{2}} {}_1F_1\left(\frac{1}{2}, \frac{3}{2}; -z\right) \\ &\overset{(a)}{=} \frac{2\Gamma\left(q+\frac{3}{2}\right)}{\sqrt{\pi}\Gamma\left(\frac{1}{2}\right)} z^{-\frac{1}{2}} {}_1F_1\left(q+\frac{3}{2}, \frac{3}{2}; -z\right), \end{aligned} \quad (12)$$

where (a) is due to the identity in [14, eq. (15.2.3)].

Thereafter, the conditional BPSK BER of UL UAV-i, i.e., $\frac{1}{2} E\left\{ g\left(SINR_i\right) \middle| \mathcal{I}, d_i^{-n} \right\}$, is evaluated as [10, eq. (2)]:

$$\begin{aligned} \frac{1}{2} E\left\{ g\left(SINR_i\right) \middle| \mathcal{I}, d_i^{-n} \right\} &\approx \frac{1}{2} \int_0^\infty \sum_{q=0}^{K_{tr}} \frac{(K_i)^q \exp(-K_i)}{\Gamma^2(q+1)} \\ &\quad \times \left(m_i[1+\mathcal{I}]\right)^{q+1} g(z) z^q \exp\left(-m_i z[1+\mathcal{I}]\right) dz \\ &\overset{(a)}{\approx} \frac{g(0)}{2} + \frac{1}{2} \int_0^\infty \sum_{q=0}^{K_{tr}} \frac{(K_i)^q \exp(-K_i)}{\Gamma^2(q+1)} g_{q+1}(z) \exp(-m_i z) \\ &\quad \times \left(\prod_{j=i+1}^{N_U} \exp(-m_i z X_j d_j^{-n}) \right) \left(\prod_{k=1}^{N_B} \exp(-m_i z Y_k U_k^{-n}) \right) dz, \end{aligned} \quad (13)$$

where (a) is result of applying integration by parts $q+1$ times.

The proof is completed after averaging (13) with respective PDFs of $X_j, Y_k, d_i^{-n}, d_j^{-n}, U_k^{-n}$.

Appendix B
Proof of Theorem 4

To begin, we invoke [11, eq. (5)] to express $\ln\left(1+SINR_i\right)$ as:

$$\begin{aligned} \ln\left(1+SINR_i\right) &= \int_0^\infty \frac{1}{z} \left[1 - \exp\left(-z X_i d_i^{-n}\right)\right] \\ &\quad \times \exp\left(-z \left[1 + \sum_{j=i+1}^{N_U} X_j d_j^{-n} + \sum_{k=1}^{N_B} Y_k U_k^{-n} \right] \right) dz. \end{aligned} \quad (14)$$

Then, averaging (14) with respect to the PDFs of $X_i, X_j, Y_k, d_i^{-n}, d_j^{-n}, U_k^{-n}$ yields (8), which completes the proof.

References

[1] T. Z. H. Ernest, A. S. Madhukumar, R. P. Sirigina, and A. K. Krishna, "A Hybrid-Duplex System with Joint Detection for Interference-Limited UAV Communications," *IEEE Trans. Veh. Technol.*, Jan. 2019.

[2] V. Yajnanarayana, Y.-P. E. Wang, S. Gao, S. Muruganathan, and X. L. Ericsson, "Interference mitigation methods for unmanned aerial vehicles served by cellular networks," in *2018 IEEE 5G World Forum (5GWF)*. IEEE, 2018, pp. 118–122.

[3] W. Mei and R. Zhang, "Uplink cooperative NOMA for cellular-connected UAV," *IEEE J. Sel. Topics Signal Process.*, February 2019.

[4] T. Z. H. Ernest, A. S. Madhukumar, R. P. Sirigina, and A. K. Krishna, "Outage Analysis and Finite SNR Diversity-Multiplexing Tradeoff of Hybrid-Duplex Systems for Aeronautical Communications," *IEEE Trans. Wireless Commun.*, April 2019.

[5] D. W. Matolak and R. Sun, "Air-ground channel characterization for unmanned aircraft systems part iii: The suburban and near-urban environments," *IEEE Trans. Veh. Technol*, 2017.

[6] T. Z. H. Ernest, A. S. Madhukumar, R. P. Sirigina, and A. K. Krishna, "Hybrid-Duplex Communications for Multi-UAV Networks: An Outage Probability Analysis," *IEEE Commun. Lett.*, 2019.

[7] V. V. Chetlur and H. S. Dhillon, "Downlink coverage analysis for a finite 3-d wireless network of unmanned aerial vehicles," *IEEE Trans. Commun*, vol. 65, no. 10, pp. 4543–4558, 2017.

[8] M. Afshang and H. S. Dhillon, "Fundamentals of modeling finite wireless networks using binomial point process." *IEEE Trans. Wireless Communications*, vol. 16, no. 5, pp. 3355–3370, 2017.

[9] A. Papoulis and S. U. Pillai, *Probability, Random Variables, and Stochastic Processes*. Tata McGraw-Hill Education, 1991.

[10] K. A. Hamdi, "A useful technique for interference analysis in nakagami fading," *IEEE Trans. Commun.*, vol. 55, no. 6, pp. 1120–1124, 2007.

[11] ——, "A useful lemma for capacity analysis of fading interference channels," *IEEE Trans. Commun.*, vol. 58, no. 2, pp. 411–416, February 2010.

[12] M. O. Hasna, M.-S. Alouini, A. Bastami, and E. S. Ebbini, "Performance Analysis of Cellular Mobile Systems with Successive Co-Channel Interference Cancellation," *IEEE Trans. Wireless Commun.*, vol. 2, no. 1, pp. 29–40, January 2003.

[13] N. B. Rached, A. Kammoun, M.-S. Alouini, and R. Tempone, "A unified moment-based approach for the evaluation of the outage probability with noise and interference," *IEEE Trans. Wireless Commun.*, vol. 16, no. 2, pp. 1012–1023, 2017.

[14] M. Abramowitz and I. Stegun, "Handbook of mathematical functions with formulas, graphs, and mathematical tables (applied mathematics series 55)," *National Bureau of Standards, Washington, DC*, 1964.